

Lithium isotopes in speleothems: Temperature-controlled variation in silicate weathering during glacial cycles

Philip A.E. Pogge von Strandmann^{1,2}, Anton Vaks^{2,3}, Miryam Bar-Matthews³, Avner Ayalon³, Ezekiel Jacob², and Gideon M. Henderson²

¹London Geochemistry and Isotope Centre (LOGIC), Institute of Earth and Planetary Sciences, University College London and Birkbeck, University of London, Gower Street, London, WC1E 6BT, UK.

²Department of Earth Sciences, University of Oxford, South Parks Road, Oxford, UK.

³Geological Survey of Israel, 30 Malkhey Israel Street, 9550161 Jerusalem, Israel.

Abstract

Terrestrial chemical weathering of silicate minerals is a fundamental component of the global cycle of carbon and other elements. Past changes in temperature, rainfall, ice cover, sea-level and physical erosion are thought to affect weathering but the relative impact of these controls through time remains poorly constrained. This problem could be addressed if the nature of past weathering could be constrained at individual sites. In this study, we investigate the use of speleothems as local recorders of the silicate weathering proxy, Li isotopes. We analysed $\delta^7\text{Li}$ and [Li] in speleothems that formed during the past 200 ka in two well-studied Israeli caves (Soreq and Tzavoa), as well as in the overlying soils and rocks. Leaching and mass balance of these soils and rocks show that Li is dominantly sourced from weathering of the overlying aeolian silicate soils.

Speleothem $\delta^7\text{Li}$ values are ubiquitously higher during glacials ($\sim 23\text{‰}$) than during interglacials ($\sim 10\text{‰}$), implying more congruent silicate weathering during interglacials (where “congruent” means a high ratio of primary mineral dissolution to secondary mineral formation). These records provide information on the processes controlling weathering in Israel. Consideration of possible processes causing this change of weathering congruency indicates a primary role for temperature, with higher temperatures causing more congruent weathering (lower $\delta^7\text{Li}_{\text{speleo}}$). The strong relationship observed between speleothem $\delta^7\text{Li}$ and climate at these locations suggests that Li isotopes may be a powerful tool with which to understand the local controls on weathering at other sites, and could be used to assess the distribution of weathering changes accompanying climate change, such as that of Pleistocene glacial cycles.

Keywords: weathering; glaciation; climate; lithium isotopes; temperature.

1.0 Introduction

Weathering of silicate minerals is a fundamental aspect of the global cycle of carbon and other elements and plays an important role in moderating climate and controlling ocean chemistry on long timescales. Controls on the rate and style of weathering include temperature, rainfall and the supply of fresh silicate material (West et al., 2005), but separating the relative importance of these controls over geological time has been challenging (Archer et al., 2000; Foster and Vance, 2006).

The major climate changes of Pleistocene glacial cycles likely caused changes in weathering at different scales, but are an example of the lack of adequate understanding of past weathering, with various studies predicting that

CO₂ drawdown by silicate weathering was between ~6–20% lower (Ludwig et al., 1999; Mokadem et al., 2015; Munhoven, 2002) to 250% higher (Munhoven and Francois, 1996) during the Last Glacial Maximum (LGM) than at present. Perhaps the most widely used proxy for weathering, seawater radiogenic strontium, shows no direct evidence for changing weathering during these cycles, but provides limits on maximum possible changes at a global scale (Mokadem et al., 2015; Vance et al., 2009). Similarly, studies based on Be isotopes suggest little variation in silicate weathering rates between glacial and interglacial states (von Blanckenburg et al., 2015), similar to some carbon mass balance calculations (Zeebe and Caldeira, 2008). However, it is also clear that weathering varied dramatically at the local scale on these timescales, due to different impacts by temperature, glacial grinding and sealevel changes (Frings et al., 2016). Studies of Pb isotopes in Fe-Mn crusts offshore the Laurentide ice sheet have allowed a more local approach, and suggest that chemical weathering was significantly (~2–3 times) lower during glacials than interglacials in this glaciated region (Crocket et al., 2013; Foster and Vance, 2006). Equally, authigenic phases from the Indian Ocean suggest that Himalayan weathering was up to 5 times lower during glacials (Wilson et al., 2015). Neodymium isotopes have been similarly interpreted, suggesting that Himalayan river discharge and weathering was lower in glacials (Burton and Vance, 2000; Gourlan et al., 2010). In contrast, Nd isotopes from around New Zealand suggest that weathering increased 2–10 times during glacials, due to the proximity of physically eroded material from glaciers (Cogez et al., 2015). Similarly, records from the South China Sea suggest elevated weathering fluxes during glacials due to greater continental exposure during sea-level fall (Wan et al., 2017). There is potential ambiguity in some of these interpretations, because radiogenic isotopes are

largely controlled by weathering provenance, and often cannot distinguish between weathering of silicates and carbonates. Such marine studies are also only able to assess past weathering at a limited range of locations and geographical scales. The ability to assess past weathering for particular environments from local continental records would be a powerful addition to the range of tools used to assess past weathering. Lithium isotopes are a tracer for weathering that respond solely to silicate weathering. Lithium is enriched in silicates by a factor of $\sim 10^3$ – 10^4 relative to crustal carbonates, so that, even in carbonate catchments, Li is dominated by weathering of silicate rocks (Kisakürek et al., 2005). Further, Li isotopes are not fractionated by plants or primary productivity (Pogge von Strandmann et al., 2016). The $\delta^7\text{Li}$ of primary silicate rocks defines a narrow range (~ 0 – 5‰ , Teng et al., 2004), and the high variability of $\delta^7\text{Li}$ in modern rivers and soil pore fluids (2 – 42‰ ; global mean $\sim 23\text{‰}$, (Dellinger et al., 2015; Huh et al., 1998; Pogge von Strandmann and Henderson, 2015) is due to preferential uptake of ^6Li by secondary clay minerals (e.g. phyllosilicates) during the weathering process (Pistiner and Henderson, 2003). The $\delta^7\text{Li}$ of surface water is therefore controlled by the “weathering congruency”, defined here (as is now common for Li isotope studies) as the ratio of primary mineral dissolution to secondary mineral formation, with congruent weathering leading to low $\delta^7\text{Li}$ (Dellinger et al., 2015; Pogge von Strandmann et al., 2017; Pogge von Strandmann and Henderson, 2015). Fully congruent weathering has never been observed, and rock-like $\delta^7\text{Li}$ values tend to only occur in hydrothermal waters where clay formation is limited (Pogge von Strandmann et al., 2016). Dissolved $\delta^7\text{Li}$ might also be affected by re-dissolving (isotopically light) secondary minerals, although to date this has only been reported to affect

$\delta^7\text{Li}$ in rainforest catchments with very different weathering regimes from those observed here (Clergue et al., 2015; Dellinger et al., 2015).

Lithium isotopes have been used to assess possible changes in weathering globally, though measurement of seawater carbonates (Hathorne and James, 2006; Lechler et al., 2015). They may also be a powerful tracer of local changes and the processes controlling weathering if a suitable substrate to record their variation is identified. In this study, we assess the use of speleothems (cave carbonates) as recorders of $\delta^7\text{Li}$ to provide a local record of terrestrial silicate weathering through time. Speleothems are an archive for high-resolution examination of past environmental conditions. In particular, speleothem chemistry is determined largely by drip water chemistry (Bar-Matthews et al., 1999; Vaks et al., 2006), which in turn is dominated by weathering processes occurring immediately above the cave (Ayalon et al., 1999). We have examined Li isotope ratios in speleothems from two well-studied Israeli caves, Soreq and Tzavoa, which are located in very different climate regimes: sub-humid Mediterranean and mildly-arid semi-desert climate, respectively.

2.0 Field area

Speleothems from two caves in Israel were examined: Soreq is on the western slope of the Judean Mountains, ~20 km west of Jerusalem, while Tzavoa is in the northern Negev Desert, which is a part of a larger Saharan-Arabian Desert belt (Fig. 1). A detailed description of the climate and environment of these caves is important, because it allows us to examine the precise weathering environments.

2.1 Climate setting

Soreq is located in a sub-humid Mediterranean climate, while Tzavoa is in mildly arid desert 65 km to the south-east, with a zone of semi-arid steppe between the two caves (Fig. 1C). Soreq Cave currently experiences 500 mm/yr rain, with a 19.5°C Average Annual Temperature (AAT), while Tzavoa experiences 150 mm/yr rain, with an AAT of 18.5°C, because of higher altitude (500-550m above sea-level) than Soreq (400m). During the last glacial, the temperatures in the region were 5–10°C lower than today (Affek et al., 2008; Almogi-Labin et al., 2009; McGarry et al., 2004). Higher precipitation/evaporation ratios during the last two glacial intervals led to intensive speleothem deposition in Tzavoa Cave (Vaks et al., 2006), but lack of moisture during most of interglacials led to limited interglacial speleothem deposition occurring only during Marine Isotopic Stages (MIS)-7a, MIS-5e and MIS-5a. In contrast, speleothem deposition at Soreq is fairly continuous throughout the studied time period (Bar-Matthews et al., 2003).

The major rainfall source is mid-latitude Atlantic–Mediterranean cyclones moving eastwards above the eastern Mediterranean Sea. The northern Sinai coastline therefore forms the southern limit at which rainclouds usually form, and the latter are carried to the east, leaving the southern region dry. This phenomenon causes the sharp precipitation gradient between Soreq Cave (central Israel) and Tzavoa Cave (northern Negev Desert), although the distance between them is only 65 km.

2.2 Cave settings – geology and vegetation

Soreq and Tzavoa caves are found within dolomites and limestones of the Upper Cretaceous Judea Group. The caves were likely formed between the Late Eocene and Miocene when the Judea Group was below the groundwater table.

The caves were uplifted above the groundwater table during two major tectonic phases in the Late Miocene–Pliocene, and during the Early Pleistocene (Frumkin and Fischhendler, 2005; Vaks et al., 2013b), into the unsaturated zone that enabled the formation of vadose speleothems.

The vegetation above Soreq Cave is Mediterranean maquis with low trees, bushes, shrubs and grasses, covering 50–80% of the surface (Fig. 2a). Above Tzavoa the vegetation is Irano-Turanian semi-desert grasses and shrubs covering less than 20% of the surface (Fig. 2c). Both caves are located on the slopes of mountains with relatively steep relief above the caves (5–45°, with occasional small cliffs), whereas small horizontal/moderate relief areas are found on the topographic highs above the caves.

2.3 Soils

The soil above the Soreq cave is of Mediterranean Terra-Rosa type, while above Tzavoa Cave it is of Loess type. Both soils appear as isolated pockets up to few tens of cm in depth between rock outcrops. Local soils are largely aeolian in origin, from dust transported from the Saharan Desert and nearer Northern Sinai Sand Dune Field (originating from Nile river sediments), both to the south and west of the studied caves (Crouvi et al., 2007) (Fig. 1b). Atlantic-Mediterranean cyclones transport this dust from its source into Israel, with dust fall $\sim 100\text{--}130\text{ g/m}^2\text{/yr}$ at the cave sites (Fig. 1b) (Ganor and Foner, 2001). During the last two glacial periods the research area received more dust compared to today because of the exposure of large areas of the Nile delta (Amit et al., 2011; Enzel et al., 2008), expansion of the Saharan-Arabian desert belt (Frumkin and Stein, 2004) and higher intensity SWW winds (Enzel et al., 2008). The primary mineralogy of Israeli soils in both regions tends to be similar, with around 30–40% quartz, 20–

30% calcite, ~8% K-feldspar and 7–10% plagioclase, with the remainder largely made up by fine-grained phyllosilicates (Ben-Israel et al., 2015; Crouvi et al., 2009; Sandler et al., 2015). The clay fraction at the two locations is slightly different, with Soreq dominated by illite-smectite clays (~80%) and 10–15% kaolinite, while Tzavoa consists of ~70% illite-smectite and 20–30% kaolinite (Sandler, 2013; Sandler et al., 2015).

At least 50% of the Mediterranean Terra-Rosa soil is aeolian (Yaalon, 1997), whereas the loess soils in the Negev are entirely aeolian (Crouvi et al., 2010). OSL ages of Terra-Rosa soils ~10 km to the east of Soreq Cave show that their age varies from 180–9000 years (Gadot et al., 2016), whereas the age of the loess soils in the Negev desert (Tzavoa Cave location) is 10–14 ka (Crouvi et al., 2009; Faershtein et al., 2016). The evidence therefore indicates that residence time of the soil cover (in pockets of <50 cm in depth) above Soreq Cave is less than ~10 ka, and the residence time of the thin loess soil pockets (0–15 cm) above the Tzavoa Cave is less than ~14 ka.

3.0 Methods

Speleothem samples were initially dissolved in 1M HCl, and trace element concentrations were analysed using a Thermo Scientific Element 2 ICP-MS (inductively coupled plasma mass spectrometer), by calibrating with a series of multi-element solutions. Accuracy and precision were assessed by analysis of the international reference standard JLS-1, and was within $\pm 4\%$ for major elements and $\pm 6\%$ for Li concentrations.

Most of the speleothems' chronology was based on previous studies (Bar-Matthews et al., 2003; Grant et al., 2012; Vaks et al., 2006). To refine the age

model of one speleothem's layer, 2-22-I₂, a single U-Th age determination was performed according to the method described in Vaks et al., 2013a).

Soils were sequentially leached by the Tessier method adapted by Pogge von Strandmann et al. (2013). The exchangeable fraction was extracted using 1M Na-acetate (NaOAc), and the carbonate fraction in 1M NaOAc adjusted to pH5 with acetic acid. The final silicate fraction (as well as the bulk rock) was dissolved in a standard routine of HF-HNO₃-HClO₄, followed by HNO₃ and HCl.

Following determination of [Li], between 0.05–0.25g of speleothem were dissolved in weak HCl to minimise leaching of any minor silicates in the speleothems. The amount of material dissolved was initially targeted to gain ~15ng Li, but following the use of a new-geometry cone (Le Roux, 2010), only ~5ng Li were needed. This dissolution was also analysed for trace elements by ICP-MS, specifically Al/Ca and Mn/Ca, to assess whether any silicates had been leached during dissolution. The cutoff for Al/Ca in carbonates has been calculated at 0.8 mmol/mol (Pogge von Strandmann et al., 2013), although values in this study were <0.07 mmol/mol. Li/Ca was also analysed, to compare the leaches to the 1M HCl dissolutions. There was agreement between these two Li content analyses within analytical uncertainty, demonstrating that silicates were not significantly leached during the initial HCl dissolution used for concentration analyses.

3.1 Lithium chemistry and analyses

Speleothems have low Li/Ca ratios, so a new Li isotope chemistry was developed to deal with the large amount of carbonate matrix. This was based on a scaled-up version of the weak HCl elution technique (Pogge von Strandmann et al., 2013). The first column consisted of 20ml AG50W-X12, where Li was eluted

in 1M HCl. This column separated Li from Ca, but not from Na. The second column is identical to that used in Pogge von Strandmann et al., 2013, and consisted of 1ml AG50W X-12, with Li eluted in 0.2M HCl. Leached and silicate fractions were purified by the standard 2-column method detailed elsewhere (Pogge von Strandmann and Henderson, 2015; Pogge von Strandmann et al., 2013). Given that Li isotopes are fractionated during ion chromatography, yields were tested by collecting splits before and after the Li collection bracket. Results showed that <0.1% of Li was present in these splits, suggesting that close to 100% was in the fraction collected for analysis. The total procedural blank for Li isotope analysis is ~0.02–0.05ng Li, which is insignificant compared to sample Li.

Analyses were performed on a Nu Plasma HR multi-collector ICP-MS at Oxford University, using a sample-standard bracketing system relative to the LSVEC standard. Analysis methods were identical to those described in Pogge von Strandmann and Henderson (2015). At an uptake rate of 75 $\mu\text{l}/\text{min}$, the sensitivity for a 20 ng/ml solution is ~23 pA of ^7Li using a standard type “A” cone, and 10^{-11} Ω resistors. When using the new-geometry skimmer cone (“low-mass high-abundance” cone (Le Roux, 2010)), 5ng/ml solution gives a ^7Li beam intensity of ~30pA for the same uptake rate, with a ~1.5 \times improved signal to noise ratio. A drawback of the high-intensity cone is that it is more susceptible to matrix contributions, and therefore if sample Na/Li >1.5, the samples had to be repurified (with standard cones, Na/Li <3 is acceptable).

Accuracy and external reproducibility, as assessed from seawater and USGS standards BCR-2 and SGR-1, is $31.3\pm 0.6\text{‰}$ (2sd, n=59, chemistry=59), $2.7\pm 0.4\text{‰}$ (n = 4, chemistry = 4) and $3.6\pm 0.4\text{‰}$ (n=3, chemistry=3), respectively (where “chemistry” denotes separate passes through full purification chemistry), which agrees well with other studies (Dellinger et al., 2015; Phan et al., 2016;

Pogge von Strandmann and Henderson, 2015). Standards measured using the new cones and the larger first column were identical to those processed using the standard method. Precision was also assessed from repeated analyses (including leaching and chemistry) of our in-house marl standard, which also gives a reproducibility of $\pm 0.6\text{‰}$ ($n=9$) (Pogge von Strandmann et al., 2013).

4.0 Results

4.1 Rocks and soils

All rock and soil data from cave regions are given in Table 1 and show somewhat similar behaviour. The carbonate portion of the host rocks (i.e. leached fraction) have $\delta^7\text{Li}$ values of 22.3 and 20.1‰ for Soreq and Tzavoa, respectively. In contrast, the silicate portion of the rocks have $\delta^7\text{Li}$ values of 10.2 and 6.1‰, respectively. The silicate portion of these carbonate rocks contains 95–96% of the bulk rock Li, but only comprise 1.7–3.3% of the rock by mass.

The exchangeable fractions of the soils overlying the rocks contain $\sim 0.04\%$ of the total soil Li in both caves, and have $\delta^7\text{Li}$ of 11.9–13.5‰. The carbonate fractions of the soils contain 0.04–0.13% of the total soil Li, and have $\delta^7\text{Li}$ values of 13.4–15.7‰, in keeping with the isotopically heavy compositions of marine-derived carbonate rocks. The silicate fractions in these soils contain $>99.8\%$ of the soil's Li, and have typical silicate rock $\delta^7\text{Li}$ values of 1.6–2.5‰.

4.2 Modern drip waters and precipitates

Modern drip waters from both Soreq and Tzavoa were collected in 2014. These have relatively low Li concentrations (0.45–1.66 ng/ml), and concentrations do not correlate with the observed drip rates. Lithium isotope

ratios are similar for all the drip waters in both caves, ranging from 20.3 to 23.9‰ (Supplementary table). In particular, drip waters were collected that are dripping onto recent cave carbonates precipitated onto concrete paths from the 1970s in Soreq cave. These drip waters have $\delta^7\text{Li}$ values of 22.8 to 23.9‰, 3.6–5.2‰ higher than the “speleothem” carbonate that is precipitating from them ($\delta^7\text{Li} = 18.7\text{--}19.2\text{‰}$ – Fig. 3). This fractionation factor is identical to that reported from inorganic calcite experiments, which also reported that fractionation is not dependent on temperature (Marriott et al., 2004).

4.3 Speleothems

Eleven well-dated speleothems from Soreq Cave and four speleothems from Tzavoa Cave, which cover the past 200 kyr, were studied, and display strong glacial-interglacial variability in oxygen and carbon stable isotope and trace element concentrations (Ayalon et al., 1999; Bar-Matthews et al., 2003; Vaks et al., 2006). Lithium concentrations range from 24 to 470 ng/g, and tend to be higher but more variable during glacials (Fig. 4a).

Speleothems from the two caves show similar $\delta^7\text{Li}$ behaviour, with a clear trend of higher $\delta^7\text{Li}$ during glacials, and lower $\delta^7\text{Li}$ during interglacials (Fig. 5). Soreq provides the most complete record, with speleothem $\delta^7\text{Li}$ values reaching a peak of $\sim 21\text{--}23\text{‰}$ during the maxima of the last two glaciations, minima of 9.8‰ in the Holocene, and 14.9‰ in the penultimate deglacial.

Due to lack of interglacial moisture during the last 200 ka, Tzavoa Cave has limited speleothem deposition, occurring mainly during glacials, and only in some interglacials (MIS-7a, MIS-5e and MIS-5a). Just before the penultimate

glaciation, $\delta^7\text{Li}$ values are $\sim 15\text{‰}$, and, in both glacials, isotope ratios increase to $\sim 23\text{‰}$.

In the time periods when speleothems exist concurrently in both caves (14–76 ka, and 125–168 ka), the $\delta^7\text{Li}$ values are generally within 1‰ of each other. At $\sim 125\text{--}137$ ka, though, $\delta^7\text{Li}$ values from Tzavoa are $\sim 4\text{‰}$ lower, and at 76 ka $\sim 7\text{‰}$ higher than those in Soreq. Isotopic fractionation between calcite and solution observed here (3.6–5.2‰ – see above) and experimentally ($\sim 3\text{--}5\text{‰}$) (Marriott et al., 2004) (Fig. 3), suggest drip water $\delta^7\text{Li}$ varied between $\sim 14\text{‰}$ shortly ($\sim 15\text{kyr}$) after the glacial maxima, to $\sim 27\text{‰}$ during glacials.

5.0 Discussion

5.1 Modern drip waters and carbonates

An aberration to the trend of decreasing $\delta^7\text{Li}_{\text{speleo}}$ of the last 20,000 years (Fig. 5) is modern carbonate precipitated onto concrete paths. At the time of the youngest speleothem sample, 1,700 years ago, drip waters had a $\delta^7\text{Li}$ of $\sim 14\text{‰}$ (assuming a calcite fractionation factor of 4‰ (Marriott et al., 2004)), while modern drip waters have values closer to 22‰. Modern drip waters are enriched in K and NO_3 , indicative of the effect of sewage, fertiliser (Orland et al., 2014) or industry contamination. Regional agriculture has increased significantly over the past 50–100 years (Orland et al., 2014). The modern carbonates have [Li] up to an order of magnitude higher than the 1,700 years old speleothem (Supplementary table), and fertilisers tend to be high in Li (Kisakürek et al., 2005). It is therefore probable that the modern samples have been contaminated by anthropogenic inputs, as also indicated by elevated $\delta^{13}\text{C}$ ratios (Ayalon et al., 1999; Bar-Matthews et al., 1999). Modern drip waters and

carbonates allow us, however, to confirm that the Li isotope fractionation into calcite in caves is similar to that in precipitation experiments (Fig. 3), but their $\delta^7\text{Li}_{\text{speleo}}$ values are likely not representative of the trends that characterise the rest of the 200 ka record.

5.2 Negligible input of seawater Li

Seawater is a significant contributor to the composition of Israeli rainwater (Mamane, 1987). The relative amount of contribution varies according to the element of interest and the location. Sodium is considered to be mainly sea-salt derived, and therefore Li/Na ratios of modern rainwater and speleothems can be used to determine whether significant amounts of Li have been sourced from sea-salt. Using published annual ranges for local rainwater Na concentrations ($\sim 5.3\text{--}8.1\ \mu\text{g}/\text{ml}$ (Mamane, 1987; Mamane et al., 1987)), and our analysis of modern rain at Soreq ($[\text{Li}] = 43\ \text{pg}/\text{ml}$), Li/Na mass ratios vary between 5.4×10^{-6} and 8.2×10^{-6} (seawater Li/Na = 16.5×10^{-6}). Speleothem Li/Na therefore suggests that $1.5 \pm 0.7\ \text{ng}/\text{g}$ of speleothem Li stems from rainwater ($3.0 \pm 1.3\ \text{ng}/\text{g}$ if the seawater ratio were transferred to rainwater), which is insignificant compared to the speleothem Li concentrations of 25–470 ng/g. Speleothems with the lowest $[\text{Li}]$ also tend to have low $\delta^7\text{Li}$, whereas seawater has high $\delta^7\text{Li} = 31\text{‰}$, further suggesting little sea-salt influence on speleothem Li compositions.

5.3 Source of Li: soils

The sequential leaching of the soils and host rocks showed that the exchangeable and carbonate fractions are isotopically heavy and have similar

$\delta^7\text{Li}$ values in comparable phases. The silicate (residue) fractions in the soil accounted for >99% of Li in the bulk soils, and had a $\delta^7\text{Li} \sim 1.6\text{--}2.5\text{‰}$, while the silicate fraction in the host carbonate rock accounted for >95% of the rocks' Li, with a $\delta^7\text{Li}$ of 6–10‰ (Table 1). A simple mass balance can be used to calculate the ratio of Li contained in carbonates and silicates above each cave. Typical soil thicknesses are 0.5m for Soreq and 0.15m for Tzavoa, and carbonate rock thicknesses from surface to cave-level are $\sim 30\text{m}$ for both. The rock is >98% carbonate by mass in Soreq and 97% carbonate at Tzavoa. With measured Li concentrations (Table 1), including those from the leaching experiments (which show that silicate-derived Li dominates the mass balance), this mass balance indicates that 70–78% of the total Li is in the soil silicate, 22–28% in rock silicate, and 1–2% in rock carbonate (Fig. 6). In actual fact, the amount of Li in the speleothems that derived from soil silicates is likely considerably higher, as the soils have a far greater proportion of high-activity (easily dissolvable) primary silicates than the carbonate rocks.

The relative dissolution rates of carbonates to silicates are harder to quantify, but a simple mass balance of Soreq's $^{87}\text{Sr}/^{86}\text{Sr}$ data (Bar-Matthews et al., 1999; Palchan et al., 2013) suggest $\sim 10\text{--}20\%$ of speleothem Sr comes from silicate dissolution, and that carbonates are dissolving $\sim 6\times$ faster than silicates. Given that the ratio of Sr in silicates/carbonates is $\sim 2000\times$ less than for Li, this suggests that >99.9% of Li in speleothems stems from silicate dissolution.

Overall, therefore, the speleothem Li dominantly stems from the weathering of the silicate portion of the overlying soils, which are largely aeolian, derived from the Northern Sinai and Nile Delta (mixed granitic-basaltic in origin) and from the Saharan-Arabian desert (granitic) (Ben-Israel et al., 2015; Ganor

and Foner, 2001; Palchan et al., 2013). Karst dissolution insignificantly affects the Li budgets of the drip waters and speleothems, because of the negligible amount of Li in the carbonate rocks.

5.4 Potential controls on weathering and Li isotopes

The dominance of silicate weathering to the Li supply in these speleothems allows an assessment of the processes limiting silicate weathering in these areas and on these timescales. Parameters known to control silicate weathering rates (West et al., 2005), are i) changing supply of silicate, ii) soil or weathering zone thickness, iii) water supply, iv) vegetation and v) temperature. In this list, the weathering reactions of i) and ii) are limited by supply of silicate material, while those of iii), iv) and v) are controlled by the kinetics of the chemical reactions for each controlling process. These parameters are discussed generally here, and specifically for the studied caves in Section 5.5.

- 1) If the supply of primary silicates to the soil increases (e.g. changing dust supply rate), then the ratio of primary silicate dust dissolution to secondary mineral formation will increase. This will result in an increase in $[\text{Li}]_{\text{diss}}$, and a decrease in $\delta^7\text{Li}_{\text{diss}}$ (where the subscript diss signifies the dissolved phase).
- 2) If the soil thickness (depth) increases, the overall thickness of weathering zone will increase and the water-rock interaction time also increases to allow greater secondary mineral formation, driving $\delta^7\text{Li}_{\text{diss}}$ high.
- 3) If the water supply (i.e. rainfall) increases so that water flows through the soil more quickly, then the supply of undersaturated water increases. Higher water supply would therefore promote primary rock dissolution

relative to secondary mineral formation and decrease water-rock interaction time, both of which would drive $\delta^{7}\text{Li}_{\text{diss}}$ towards lower, more rock-like, values.

- 4) It is more difficult to predict the effects of changing temperature on the congruency of weathering, because it is unknown precisely how temperature affects dissolution and the formation of secondary minerals, and the relative change of these two processes, even in weathering regimes such as here where material supply is not limiting the weathering reaction, and therefore kinetics dominate (West et al., 2005). Both natural and experimental studies have shown that dissolution rates of common silicate minerals increase 2–10% for every degree of temperature increase (once runoff effects are normalised (Eiriksdottir et al., 2013; Gislason et al., 2009)). Equally, the solubility of most (non-oxide) secondary minerals increases with temperature (Stefansson and Gislason, 2001) so that their formation is less favoured as temperature increases. These two temperature dependencies suggest that higher temperatures promote primary mineral dissolution relative to secondary mineral formation. Riverine fluxes of other elements that are affected by secondary mineral formation, such as Ca or Mg, confirm this, with discharge-normalised fluxes increasing with temperature. This increase is less pronounced for Na, which is much less impacted by secondary mineral formation (Eiriksdottir et al., 2013; Gislason et al., 2009), suggesting that the temperature dependence is driven by both primary mineral dissolution and secondary mineral formation. Higher temperature is therefore expected to increase the congruency of weathering, leading to less removal of isotopically light Li into secondary

minerals (Pistiner and Henderson, 2003; Vigier et al., 2008; Wimpenny et al., 2015; Wimpenny et al., 2010), and therefore a lower $\delta^7\text{Li}_{\text{diss}}$.

In summary, thicker soil is expected to increase $\delta^7\text{Li}_{\text{diss}}$, while increased rainfall, silicate supply, or temperature should decrease it.

5.5 Determining the controls on Israeli $\delta^7\text{Li}$ and weathering

The theoretical controls on $\delta^7\text{Li}$ discussed in the previous section, combined with the well-understood field area of this study, allows us to determine the processes controlling changes in weathering conditions at this location during the last two glacial cycles. The process(es) controlling Li fractionation must explain the more incongruent weathering (i.e. higher $\delta^7\text{Li}_{\text{speleo}}$) experienced during glacial periods, and the general similarity of the two cave records relative to one another despite their different settings and secondary mineralogy in the modern (Sandler, 2013; Sandler et al., 2015), where it must also be stressed that variations in primary mineralogy in both settings is less important, as they have a very narrow range in $\delta^7\text{Li}$.

There is also a glacial-to-interglacial difference in [Li] in the two caves (Fig 4), though not as clear as that for $\delta^7\text{Li}$. The controls on trace-metal concentrations in speleothems have been extensively studied (e.g. Day and Henderson, 2013; Fairchild and Treble, 2009) and, although Li has not been amongst the trace elements typically measured, controls on speleothem Li/Ca can be assessed by analogy with other elements. For elements with a low partition coefficient into carbonate, including Li and frequently measured elements such as Mg, Sr and Ba, a dominant control is often the amount of calcite

precipitated from karst waters before they reach the speleothem growth surface (i.e. prior-calcite precipitation). This process would be expected to yield higher Li/Ca during dry periods, which is the opposite to that observed. For [Li] there is also an inverse dependence of partitioning into carbonate with temperature (Marriott et al., 2004). Glacial temperatures were $\sim 10^{\circ}\text{C}$ colder than interglacials at Soreq (Affek et al., 2008) which would be expected to lead to Li/Ca $\sim 2\times$ higher in the glacials, possibly explaining much of the change in Li/Ca. Weathering changes (e.g. dust supply) may also contribute to changes in Li/Ca with time, but will be only one of several processes influencing the ratio. This highlights the advantage of Li isotopes as a specific tracer for weathering. Prior-calcite-precipitation is not expected to generate large change in $\delta^7\text{Li}$, and there is no dependency of $\delta^7\text{Li}$ with temperature (Marriott et al., 2004), so that weathering changes are expected to be the dominant control on $\delta^7\text{Li}$.

5.5.1 Supply of silicate

The relatively short residence time ($<10\text{--}14\text{ ka}$ – Section 2.3) of the present soils means it is theoretically possible that changing glacial-interglacial aeolian supply could control the observed $\delta^7\text{Li}_{\text{speleo}}$ signals. However, an increased dust supply, which in Israel occurred during the glacials (Crouvi et al., 2009; Enzel et al., 2008), would decrease $\delta^7\text{Li}_{\text{diss}}$ by providing fresh mineral surfaces. This is the opposite from the observed trend (Fig. 5), implying that the changes in weathering recorded by $\delta^7\text{Li}_{\text{speleo}}$ variations are not limited by dust supply variations.

Further, at present and over the past three interglacials, Soreq has received smaller amounts of dust than Tzavoa, because of its greater distance

from the source (Crouvi et al., 2008; Enzel et al., 2008; Ganor and Foner, 2001). Soreq only received similar dust to Tzavoa during glacial periods when sea level decreased, and the northern coast of Sinai was located a few tens of km further to the north (Enzel et al., 2008) (Fig. 1b). The similarity in $\delta^7\text{Li}_{\text{speleo}}$ between the two caves therefore argues against a regime in which weathering reactions are limited by supply of silicate dust.

5.5.2 Soil thickness

The thickness of the soil above the caves is primarily a function of the dust supply (see above) and removal by erosion and chemical weathering. There is little soil accumulation on the modern hill-slopes (except in isolated pockets), but more so on the flatter hill-tops (e.g. Fig. 2b). Soils were thought to be thicker in the last glacial than at present (Faershtein et al., 2016). Thicker soils would increase $\delta^7\text{Li}_{\text{diss}}$, meaning that higher $\delta^7\text{Li}_{\text{speleo}}$ in the glacials (as observed) could suggest a soil thickness control on $\delta^7\text{Li}_{\text{diss}}$ and silicate weathering. However, the timing of dust fluxes in the region does not agree with the observed $\delta^7\text{Li}_{\text{speleo}}$ patterns: dust fluxes started increasing at 95 ka, thickening soil cover during the glacials (Crouvi et al., 2008), while Soreq has approximately constant $\delta^7\text{Li}_{\text{speleo}}$ from ~128 to 68 ka (Fig. 5). In addition, the timing of loess buildup and loss in the Negev highlands during the last glacial period does not correspond to Tzavoa's $\delta^7\text{Li}_{\text{speleo}}$ pattern. Soil thickness there increased from ~95 ka until 28 ka, after which loess supply decreased and erosion washed the soil into the valleys (Crouvi et al., 2008; Faershtein et al., 2016). By 24 ka, the colluvium was exposed, which was eroded along with the underlying sediment, with extensive incision occurring towards the end of that time period (Faershtein et al., 2016).

However, from ~ 33 to 14 ka, $\delta^{7}\text{Li}_{\text{speleo}}$ values in Tzavoa are unchanged (Fig. 5). Hence, while the generally greater soil thickness during the glacials would drive solution $\delta^{7}\text{Li}_{\text{diss}}$ higher (as observed), the detail in timing between evidence of soil thickness and $\delta^{7}\text{Li}$ suggests that the former is not significantly controlling the latter. In MIS-5e, however, Tzavoa generally has lower $\delta^{7}\text{Li}_{\text{speleo}}$ than Soreq by $\sim 4\text{‰}$. This might be explained by vegetative stabilisation of soil cover above Soreq Cave, leading to thicker soils than those above Tzavoa (see 5.5.4) during this period only.

5.5.3 Rainfall

Influx from rainfall was higher at both caves during glacials (Ayalon et al., 1999; Vaks et al., 2006), which is expected to lower $\delta^{7}\text{Li}_{\text{diss}}$, the opposite from that observed. Further, Soreq cave was always wetter than Tzavoa, because of Tzavoa's remoteness from the Mediterranean storm tracks (Vaks et al., 2006), but the two caves have similar $\delta^{7}\text{Li}_{\text{speleo}}$ values (Fig. 5). This suggests that water supply was not limiting silicate weathering.

5.5.4 Vegetation

The same argument also applies to vegetation. Soreq is more vegetated than Tzavoa, but the similar $\delta^{7}\text{Li}_{\text{speleo}}$ behaviour implies that vegetation is not limiting weathering. In MIS-5e, however, Tzavoa generally has lower $\delta^{7}\text{Li}_{\text{speleo}}$ than Soreq by $\sim 4\text{‰}$. Vegetative stabilisation of soil thickness may play a role here, as Soreq has thicker, more stable, soils.

5.5.5 Temperature

The final potential control on Li isotopes and weathering in these regions is temperature. Lower temperatures during glacials could explain the higher $\delta^7\text{Li}_{\text{speleo}}$ values observed at both caves during these periods, and the similar temperatures at the two caves can explain the similar $\delta^7\text{Li}_{\text{speleo}}$ between them. Palaeo-temperatures have been determined from Soreq and the marine record from three separate studies, using clumped isotopes (Affek et al., 2008) and fluid inclusions from Soreq (McGarry et al., 2004) and alkenones from a nearby marine core (Almogi-Labin et al., 2009). There is a strong correlation between temperature and speleothem $\delta^7\text{Li}$, with lower $\delta^7\text{Li}_{\text{speleo}}$ values at higher temperatures (Fig. 7), further supporting the importance of temperature in controlling the observed $\delta^7\text{Li}$ change. This variability cannot be caused by a temperature-controlled change in the fractionation of Li isotopes during growth of secondary minerals, because the temperature dependence of this fractionation is small (Vigier et al., 2008) and, with the observed temperature change, would only cause a 0.1–1.7‰ change in fractionation. Instead, this implies that silicate weathering is more congruent when temperatures are higher, due to a temperature-control on both primary and secondary mineral solubility, as discussed in Section 5.4.

5.6 Implications for silicate weathering

For a given isotopic fractionation factor during secondary mineral formation, the fraction of Li in solution relative to that incorporated into secondary minerals (f_w) can be calculated using the formula (Pogge von Strandmann et al., 2012):

$$d_w^i = d_w^j + 1000(a - 1) \times \ln(f_w)$$

where δ_w is the $\delta^7\text{Li}$ of water (i.e. corrected for uptake into calcite), and δ_w^i is the starting composition (i.e. the $\delta^7\text{Li}$ of the host soils). In this case, we use the fractionation factor $\alpha = 0.98$, which is the difference between modern drip waters and silicate fractions of the overlying soils. Notably, using this fractionation factor requires a Rayleigh relationship, as equilibrium could not cause the observed amount of fractionation for this fractionation factor. This shows that the amount of Li in solution was on average 25% greater during interglacials than glacials, and was almost twice as great shortly after deglaciation, compared to glacial maxima (Fig. 8).

The implication is that the silicate weathering congruency or efficiency (lithium released per unit of silicate rock (Pogge von Strandmann et al., 2016; Pogge von Strandmann and Henderson, 2015)) was higher during interglacials. This can also be extrapolated to the cations that play a significant role in the carbon cycle, calcium and magnesium. Both are affected by secondary mineral formation and sorption similarly to Li, and, in basaltic weathering regimes where quantification is relatively straightforward, are as mobile as Li within a factor of 2–4 (Pogge von Strandmann et al., 2016). In contrast, quantifying these mobilities during granite weathering is not yet possible, given a lack of data. Hence, in these soils that are mixtures of basaltic and granitic dust, Li isotopes provide a qualitative measure of the efficiency of CO_2 sequestration, but further work is required before they can be quantitatively related to the trapping of Ca and Mg in continental clays.

Overall, therefore, because more congruent weathering ultimately results in less cations sequestered into secondary minerals, the data imply that CO₂ drawdown efficiency (unit CO₂ sequestered per unit silicate rock) in these semi-arid areas of Israel was greater in interglacials. While it is difficult to calculate weathering rates directly from Li isotopes (Pogge von Strandmann et al., 2017), weathering processes in this area appear to be responding to a climatic control. Determining the effect on global seawater is difficult, because different signals may counteract each other, creating less variability in seawater (Foster and Vance, 2006; von Blanckenburg et al., 2015). Hence, seawater and its archives may be less useful in examining weathering over relatively short timescales than continental records such as speleothems.

6.0 Conclusions

This study has analysed Li isotope ratios from speleothems, which formed during the last 200kyr in two Israeli caves distinct in their modern climates, Soreq and Tzavoa, as well as accompanying rocks, soils and drip waters. The goal was to test the use of speleothems as an archive to capture the silicate weathering proxy, $\delta^7\text{Li}$, and to assess local controls on silicate weathering in a continental archive, rather than using marine records which average over broad geographical regions (or globally). Such local records are critical in assessing the processes that control weathering, and hence how weathering alters with climate change.

Host-rock and soils analysis shows that Li stems from weathering of soils composed of aeolian silicates. The speleothem Li isotopes show a ubiquitous trend of lower $\delta^7\text{Li}_{\text{speleo}}$ values during interglacials, with the most rapid decrease immediately after the two sampled deglaciations. The pattern of change and

absolute $\delta^{7}\text{Li}_{\text{speleo}}$ values are very similar in the two caves. The $\delta^{7}\text{Li}$ changes cannot readily be explained by changes in dust supply or soil thickness (except possibly during interglacial MIS-5.5). Instead, $\delta^{7}\text{Li}_{\text{speleo}}$ variations are explained by temperature change, with which they correlate well. Lower $\delta^{7}\text{Li}_{\text{speleo}}$ correlates with higher temperatures of the interglacials. This suggests that primary rock dissolution is enhanced relative to secondary mineral formation as temperatures increase, in agreement with modern weathering studies. The data indicate the potential for use of $\delta^{7}\text{Li}$ analysis in speleothems to assess past weathering, and show that, for this Israeli semi-arid region, silicate weathering becomes more congruent at higher temperatures.

Acknowledgements

Yuval Burstyn is thanked for collecting drip waters, soils and recent carbonates. The Israel Nature and Parks Authority is thanked for sampling permits. Phil Holdship is thanked for assistance with concentration analyses. Analyses and PPvS were funded by NERC advanced fellowship NE/I020571/2 and ERC Consolidator grant 682760 - CONTROLPASTCO2, while some additional analyses were funded by NERC fellowship NE/G013829/1. This manuscript was improved by reviews from Friedhelm von Blanckenburg and two anonymous reviewers.

References

Affek, H.P., Bar-Matthews, M., Ayalon, A., Matthews, A., Eiler, J.M., 2008. Glacial/interglacial temperature variations in Soreq cave speleothems as

recorded by 'clumped isotope' thermometry. *Geochim. Cosmochim. Acta* 72, 5351–5360.

Almogi-Labin, A., Bar-Matthews, M., Shriki, D., Kolosovsky, E., Paterne, M., Schilman, B., Ayalon, A., Aizenshtat, Z., Matthews, A., 2009. Climatic variability during the last ~90 ka of the southern and northern Levantine Basin as evident from marine records and speleothems. *Quaternary Science Reviews* 28, 2882–2896.

Amit, R., Enzel, Y., Crouvi, O., Simhai, O., Matmon, A., Porat, N., McDonald, E., Gillespie, A.R., 2011. The role of the Nile in initiating a massive dust influx to the Negev late in the middle Pleistocene. *Geol. Soc. Am. Bull.* 123, 873–889.

Archer, D., Winguth, A., Lea, D.W., Mahowald, N., 2000. What causes the glacial/interglacial atmospheric pCO₂ cycles? *Rev. Geophys.* 38, 159–189.

Ayalon, A., Bar-Matthews, M., Kaufman, A.J., 1999. Petrography, strontium, barium and uranium concentrations, and strontium and uranium isotope ratios in speleothems as palaeoclimatic proxies: Soreq Cave, Israel. *The Holocene* 9, 715–722.

Bar-Matthews, M., Ayalon, A., Gilmour, M., Matthews, A., Hawkesworth, C.J., 2003. Sea-land oxygen isotopic relationships from planktonic foraminifera and speleothems in the Eastern Mediterranean region and their implication for paleorainfall during interglacial intervals. *Geochim. Cosmochim. Acta* 67, 3181–3199.

Bar-Matthews, M., Ayalon, A., Kaufman, A.J., Wasserburg, G.J., 1999. The Eastern Mediterranean paleoclimate as a reflection of regional events: Soreq cave, Israel. *Earth Planet. Sci. Lett.* 166, 85–95.

Ben-Israel, M., Enzel, Y., Amit, R., Erel, Y., 2015. Provenance of the various grain-size fractions in the Negev loess and potential changes in major dust sources to the Eastern Mediterranean. *Quaternary Research* 83, 105–115.

Burton, K.W., Vance, D., 2000. Glacial-interglacial variations in the neodymium isotope composition of seawater in the Bay of Bengal recorded by planktonic foraminifera. *Earth Planet. Sci. Lett.* 176, 425–441.

Clergue, C., Dellinger, M., Buss, H.L., Gaillardet, J., Benedetti, M.F., Dessert, C., 2015. Influence of atmospheric deposits and secondary minerals on Li isotopes budget in a highly weathered catchment, Guadeloupe (Lesser Antilles). *Chem. Geol.* 414, 28–41.

Cogez, A., Meynadier, L., Allegre, C.J., Limmois, D., Herman, F., Gaillardet, J., 2015. Constraints on the role of tectonic and climate on erosion revealed by two time series analysis of marine cores around New Zealand. *Earth Planet. Sci. Lett.* 410, 174–185.

Crocket, K.C., Foster, G.L., Vance, D., Richards, D.A., Tranter, M., 2013. A Pb isotope tracer of ocean-ice sheet interaction: the record from the NE Atlantic during the Last Glacial/Interglacial cycle. *Quaternary Science Reviews* 82, 133–144.

Crouvi, O., Amit, R., Enzel, Y., Gillespie, A.R., 2010. Active sand seas and the formation of desert loess. *Quaternary Science Reviews* 29, 2087–2098.

Crouvi, O., Amit, R., Enzel, Y., Porat, N., McDonald, E.V., 2007. Regional pedosedimentary stratigraphic units in the primary eolian loess of the Negev Desert, Israel, in: Crouvi, O., Malik, U., Oren, O., Shalev, E., Friedman, V., Yechieli, Y. (Eds.), *Israel Geological Society, Annual Meeting: Neven Zohar, The Dead Sea*.

Crouvi, O., Amit, R., Enzel, Y., Porat, N., Sandler, A., 2008. Sand dunes as a major proximal dust source for late Pleistocene loess in the Negev desert, Israel. *Quaternary Research* 70, 275–282.

- Crouvi, O., Amit, R., Porat, N., Gillespie, A.R., McDonald, E.V., Enzel, Y., 2009. Significance of primary hilltop loess in reconstructing dust chronology, accretion rates, and sources: An example from the Negev Desert, Israel. *Journal of Geophysical Research* 114, F0217.
- Day, C.C., Henderson, G.M., 2013. Controls on Trace-element Partitioning in Cave-analogue Calcite. *Geochim. Cosmochim. Acta* 120, 612–627.
- Dellinger, M., Gaillardet, J., Bouchez, J., Calmels, D., Louvat, P., Dosseto, A., Gorge, C., Alanoca, L., Maurice, L., 2015. Riverine Li isotope fractionation in the Amazon River basin controlled by the weathering regimes. *Geochim. Cosmochim. Acta* 164, 71–93.
- Eiriksdottir, E.S., Gislason, S.R., Oelkers, E.H., 2013. Does temperature or runoff control the feedback between chemical denudation and climate? Insights from NE Iceland. *Geochim. Cosmochim. Acta* 107, 65–81.
- Enzel, Y., Amit, R., Dayan, U., Crouvi, O., Kahana, R., Ziv, B., Sharon, D., 2008. The climatic and physiographic controls of the eastern Mediterranean over the late Pleistocene climates in the southern Levant and its neighboring deserts. *Glob. Planet. Change* 60, 165-192.
- Faershtein, G., Porat, N., Avni, Y., Matmon, A., 2016. Aggradation–incision transition in arid environments at the end of the Pleistocene: An example from the Negev Highlands, southern Israel. *Geomorphology* 253, 289-304.
- Fairchild, I.J., Treble, P.C., 2009. Trace Elements in Speleothems As Recorders of Environmental Change. *Quaternary Science Reviews* 28.
- Foster, G.L., Vance, D., 2006. Negligible glacial-interglacial variation in continental chemical weathering rates. *Nature* 444, 918-921.
- Frings, P.J., Clymans, W., Fontorbe, G., De la Rocha, C.L., Conley, D.J., 2016. The continental Si cycle and its impact on the ocean Si isotope budget. *Chem. Geol.* 425, 12–36.
- Frumkin, A., Fischhendler, I., 2005. Morphometry and distribution of isolated caves as a guide for phreatic and confined paleohydrological conditions. *Geomorphology* 67, 457-471.
- Frumkin, A., Stein, M., 2004. The Sahara-East Mediterranean dust and climate connection revealed by strontium and uranium isotopes in a Jerusalem speleothem. *Earth Planet. Sci. Lett.* 217, 451-464.
- Gadot, Y., Davidovich, U., Avni, G., Avni, Y., Piasezky, M., Faershtein, G., Golan, D., Porat, N., 2016. The formation of a Mediterranean terraced landscape: Mount Eitan, Judean Highlands, Israel. *Journal of Archaeological Science: Reports* 6, 397-417.
- Ganor, E., Foner, H.A., 2001. Mineral dust concentrations, deposition fluxes and deposition velocities in dust episodes over Israel. *Journal of Geophysical Research* 106, 18431-18437.
- Gislason, S.R., Oelkers, E.H., Eiriksdottir, E.S., Kardjilov, M.I., Gisladottir, G., Sigfusson, B., Snorrason, A., Elefsen, S., Hardardottir, J., Torssander, P., Oskarsson, N., 2009. Direct evidence of the feedback between climate and weathering. *Earth Planet. Sci. Lett.* 277, 213-222.
- Gourlan, A.T., Meynadier, L., Allegre, C.J., Tapponnier, P., Birck, J.L., Joron, J.-L., 2010. Northern Hemisphere climate control of the Bengali rivers discharge during the past 4 Ma. *Quaternary Science Reviews* 29, 2484–2498.
- Grant, K.M., Rohling, E.J., Bar-Matthews, M., Ayalon, A., Medina-Elizalde, M., Ramsey, C.B., Satow, C., Roberts, A.P., 2012. Rapid coupling between ice volume and polar temperature over the past 150,000 years. *Nature* 491, 744-747.

Hathorne, E.C., James, R.H., 2006. Temporal record of lithium in seawater: a tracer for silicate weathering? *Earth Planet. Sci. Lett.* 246, 393–406.

Huh, Y., Chan, L.H., Zhang, L., Edmond, J.M., 1998. Lithium and its isotopes in major world rivers: Implications for weathering and the oceanic budget. *Geochim. Cosmochim. Acta* 62, 2039–2051.

Kisakürek, B., James, R.H., Harris, N.B.W., 2005. Li and $\delta^7\text{Li}$ in Himalayan rivers: Proxies for silicate weathering? *Earth Planet. Sci. Lett.* 237, 387–401.

Le Roux, P.J., 2010. Lithium isotope analysis of natural and synthetic glass by laser ablation MC-ICP-MS. *J. Anal. At. Spectrom.* 25, 1033–1038.

Lechler, M., Pogge von Strandmann, P.A.E., Jenkyns, H.C., Prosser, G., Parente, M., 2015. Lithium-isotope evidence for enhanced silicate weathering during OAE 1a (Early Aptian Selli event). *Earth Planet. Sci. Lett.* 432, 210–222.

Ludwig, W., Amiotte-Suchet, P., Probst, J.-L., 1999. Enhanced chemical weathering of rocks during the last glacial maximum: a sink for atmospheric CO₂? *Chem. Geol.* 159, 147–161.

Mamane, Y., 1987. Chemistry of precipitation in Israel. *Sci. Total Environ.* 61, 1–13.

Mamane, Y., Dayan, U., Miller, J.M., 1987. Contribution of alkaline and acidic sources to precipitation in Israel. *Sci. Total Environ.* 61, 15–22.

Marriott, C.S., Henderson, G.M., Crompton, R., Staubwasser, M., Shaw, S., 2004. Effect of mineralogy, salinity, and temperature on Li/Ca and Li isotope composition of calcium carbonate. *Chem. Geol.* 212, 5–15.

McGarry, S., Bar-Matthews, M., Matthews, A., Vaks, A., Schilman, B., Ayalon, A., 2004. Constraints on hydrological and paleotemperature variations in the Eastern Mediterranean region in the last 140 ka given by the δD values of speleothem fluid inclusions. *Quaternary Science Reviews* 23, 919–934.

Mokadem, F., Parkinson, I.J., Hathorne, E.C., Anand, P., Allen, J.T., Burton, K.W., 2015. High-precision radiogenic strontium isotope measurements of the modern and glacial ocean: Limits on glacial–interglacial variations in continental weathering. *Earth Planet. Sci. Lett.* 415, 111–120.

Munhoven, G., 2002. Glacial-interglacial changes of continental weathering: estimates of the related CO₂ and HCO₃⁻ flux variations and their uncertainties. *Glob. Planet. Change* 33, 155–176.

Munhoven, G., Francois, L.M., 1996. Glacial-interglacial variability of atmospheric CO₂ due to changing continental silicate rock weathering: A model study. *J. Geophys. Res.-Atmos.* 101, 21423–21437.

Orland, I.J., Burstyn, Y., Bar-Matthews, M., Kozdon, R., Ayalon, A., Matthews, A., Valley, J.W., 2014. Seasonal climate signals (1990–2008) in a modern Soreq Cave stalagmite as revealed by high-resolution geochemical analysis. *Chem. Geol.* 363, 322–333.

Palchan, D., Stein, M., Almogi-Labin, A., Erel, Y., Goldstein, S.L., 2013. Dust transport and synoptic conditions over the Sahara–Arabia deserts during the MIS6/5 and 2/1 transitions from grain-size, chemical and isotopic properties of Red Sea cores. *Earth Planet. Sci. Lett.* 382, 125–139.

Phan, T.T., Capo, R.C., Stewart, B.W., Macpherson, G.L., Rowan, E.L., Hammack, R.W., 2016. Factors controlling Li concentration and isotopic composition in formation waters and host rocks of Marcellus Shale, Appalachian Basin. *Chem. Geol.* 420, 162–179.

Pistiner, J.S., Henderson, G.M., 2003. Lithium-isotope fractionation during continental weathering processes. *Earth Planet. Sci. Lett.* 214, 327–339.

- Pogge von Strandmann, P.A.E., Burton, K.W., Opfergelt, S., Eiriksdottir, E.S., Murphy, M.J., Einarsson, A., Gislason, S.R., 2016. The effect of hydrothermal spring weathering processes and primary productivity on lithium isotopes: Lake Myvatn, Iceland. *Chem. Geol.* in press.
- Pogge von Strandmann, P.A.E., Frings, P.J., Murphy, M.J., 2017. Lithium isotope behaviour during weathering in the Ganges Alluvial Plain. *Geochim. Cosmochim. Acta* 198, 17–31.
- Pogge von Strandmann, P.A.E., Henderson, G.M., 2015. The Li isotope response to mountain uplift. *Geology* 43, 67–70.
- Pogge von Strandmann, P.A.E., Jenkyns, H.C., Woodfine, R.G., 2013. Lithium isotope evidence for enhanced weathering during Oceanic Anoxic Event 2. *Nature Geoscience* 6, 668–672.
- Pogge von Strandmann, P.A.E., Opfergelt, S., Lai, Y.J., Sigfusson, B., Gislason, S.R., Burton, K.W., 2012. Lithium, magnesium and silicon isotope behaviour accompanying weathering in a basaltic soil and pore water profile in Iceland. *Earth Planet. Sci. Lett.* 339–340, 11–23.
- Sandler, A., 2013. Clay distribution over the landscape of Israel: From the hyper-arid to the Mediterranean climate regimes. *Catena* 110, 119–132.
- Sandler, A., Meunier, A., Velde, B., 2015. Mineralogical and chemical variability of mountain red/brown Mediterranean soils. *Geoderma* 239–240, 156–167.
- Stefansson, A., Gislason, S.R., 2001. Chemical weathering of basalts, Southwest Iceland: Effect of rock crystallinity and secondary minerals on chemical fluxes to the ocean. *Am. J. Sci.* 301, 513–556.
- Teng, F.Z., McDonough, W.F., Rudnick, R.L., Dalpe, C., Tomascak, P.B., Chappell, B.W., Gao, S., 2004. Lithium isotopic composition and concentration of the upper continental crust. *Geochim. Cosmochim. Acta* 68, 4167–4178.
- Vaks, A., Bar-Matthews, M., Ayalon, A., Matthews, A., Frumkin, A., Dayan, U., Halicz, L., Almogi-Labin, A., Schilman, B., 2006. Paleoclimate and location of the border between Mediterranean climate region and the Saharo-Arabian Desert as revealed by speleothems from the northern Negev Desert, Israel. *Earth Planet. Sci. Lett.* 249, 384–399.
- Vaks, A., Gutareva, O.S., Breitenbach, S.F.M., Avirmed, E., Mason, A.J., Thomas, A.L., Osinzev, A.V., Kononov, A.M., Henderson, G.M., 2013a. Speleothems Reveal 500,000-Year History of Siberian Permafrost. *Science* 340 183–186.
- Vaks, A., Woodhead, J., Bar-Matthews, M., Ayalon, A., Cliff, R.A., Zilberman, T., Matthews, A., Frumkin, A., 2013b. Pliocene–Pleistocene climate of the northern margin of Saharan–Arabian Desert recorded in speleothems from the Negev Desert, Israel. *Earth Planet. Sci. Lett.* 368, 88–100.
- Vance, D., Teagle, D.A.H., Foster, G.L., 2009. Variable Quaternary chemical weathering fluxes and imbalances in marine geochemical budgets. *Nature* 458, 493–496.
- Vigier, N., Decarreau, A., Millot, R., Carignan, J., Petit, S., France-Lanord, C., 2008. Quantifying Li isotope fractionation during smectite formation and implications for the Li cycle. *Geochim. Cosmochim. Acta* 72, 780–792.
- von Blanckenburg, F., Bouchez, J., Ibarra, D.E., Maher, K., 2015. Stable runoff and weathering fluxes into the oceans over Quaternary climate cycles. *Nature Geoscience* 8, 538–542.
- Wan, S., Clift, P.D., Zhao, D., Hovius, N., Munhoven, G., France-Lanord, C., Wang, Y., Xiong, Z., Huang, J., Yu, Z., Zhang, J., Ma, W., G., Z., Li, A., Li, T., 2017. Enhanced silicate weathering of tropical shelf sediments exposed during glacial lowstands: A sink for atmospheric CO₂. *Geochim. Cosmochim. Acta* 200, 123–144.

- West, A.J., Galy, A., Bickle, M., 2005. Tectonic and climatic controls on silicate weathering. *Earth Planet. Sci. Lett.* 235, 211–228.
- Wilson, D.J., Galy, A., Piotrowski, A.M., Banakar, V.K., 2015. Quaternary climate modulation of Pb isotopes in the deep Indian Ocean linked to the Himalayan chemical weathering. *Earth Planet. Sci. Lett.* 424, 256–268.
- Wimpenny, J., Colla, C.A., Yu, P., Yin, Q.Z., Rustad, J.R., Casey, W.H., 2015. Lithium isotope fractionation during uptake by gibbsite. *Geochim. Cosmochim. Acta* 168, 133–150.
- Wimpenny, J., Gislason, S.R., James, R.H., Gannoun, A., Pogge von Strandmann, P.A.E., Burton, K.W., 2010. The behaviour of Li and Mg isotopes during primary phase dissolution and secondary mineral formation in basalt. *Geochim. Cosmochim. Acta* 74, 5259–5279.
- Yaalon, D.H., 1997. Soils in the Mediterranean region: what makes them different? *Catena* 28, 157–169.
- Zeebe, R.E., Caldeira, K., 2008. Close mass balance of long-term carbon fluxes from ice-core CO₂ and ocean chemistry records. *Nature Geoscience* 1, 312–315.

	$\delta^7\text{Li}$	2sd	Li ($\mu\text{g/g}$)	fLi (by total rock mass)
Soreq				
<i>Rock</i>				
Carbonate	22.3	0.5	0.05	0.05
Residue	10.2	0.1	49.7	0.95
Bulk rock	9.4	0.3	46.3	
<i>Soil</i>				
Exchangeable	13.5	0.3	0.01	0.0004
Carbonate	15.7	0.5	0.01	0.0004
Residue	1.6	0.2	31.7	0.9993
Bulk	1.6	0.4	32.0	
Tzavoa				
<i>Rock</i>				
Carbonate	20.1	0.2	0.06	0.04
Residue	6.1	0.4	42.5	0.96
Bulk rock	7.4	0.4	38.2	
<i>Soil</i>				
Exchangeable	11.9	0.2	0.01	0.0004
Carbonate	13.4	0.4	0.03	0.0013
Residue	2.5	0.8	22.5	0.9983
Bulk	3.2	0.2	22.9	

Table 1. Data from sequential extraction of the overlying soils and rocks. The fraction of Li by total rock mass (f_{Li}) was calculated from the mass of original material lost during the leaching steps, and the measured Li abundance in the individual phases (see text for details).

Figure 1

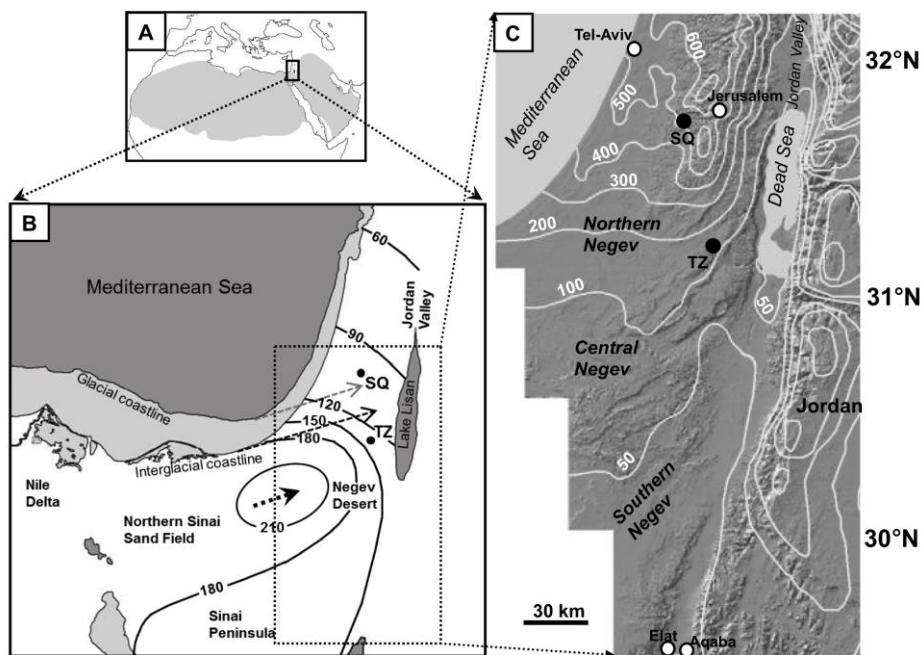


Figure 1. (A) Geographical position of the research area. Saharan-Arabian Desert is shown in grey; (B) Glacial and interglacial positions of Sinai and Nile Delta coast (Enzel et al., 2008), and the expected northward shift in location of the dust plume. The present day dustfall map (g/m^2 per year)(Ganor and Foner, 2001) is shown by black contours, whereas the two studied caves, Tzavoa (TZ) and Soreq (SQ) are shown as well. Thick and short arrow shows the W-S-W direction of strong winds, blowing in the area during the passage of winter storms (Atlantic-Mediterranean cyclones). Two thin arrows show how the dustfall contours may

shift northward with the shift of the coastline from interglacial (black arrow) to glacial position (grey arrow), with the same wind intensity. Lake Lisan shown on the map is a Last Glacial precursor of the Dead Sea; (C) Precipitation map of the research area with the locations of the two caves (Vaks et al., 2006).

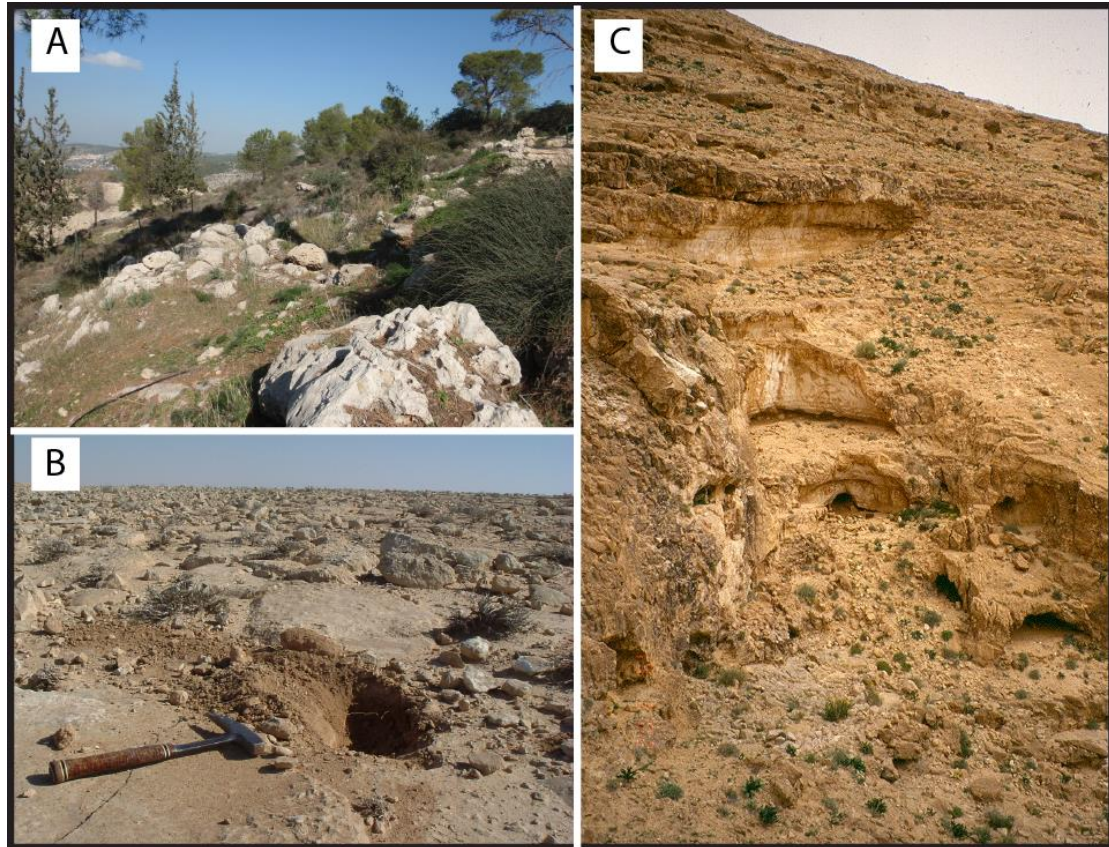


Figure 2. A) topography and vegetation above Soreq Cave; B) sampling of a soil pocket above Tzavoa Cave; C) topography and vegetation at the entrance of Tzavoa Cave (Photo by A. Frumkin).

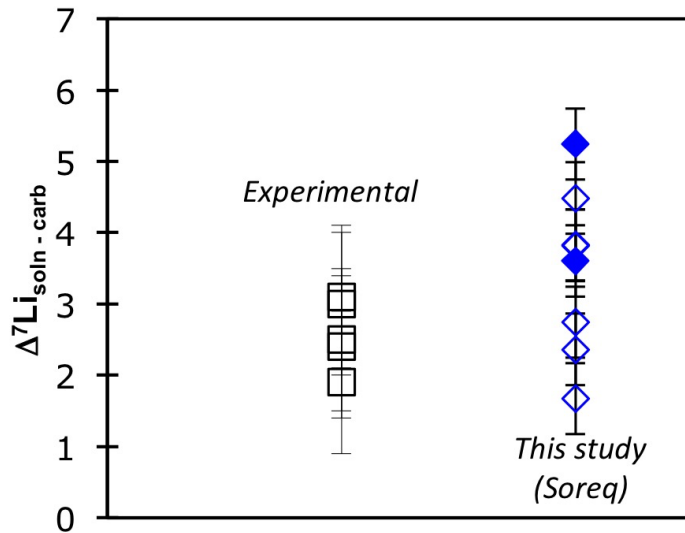


Figure 3. The Li isotopic difference between carbonate and solution for modern drip waters and carbonates (this study) and experimental carbonates (Marriott et al., 2004). For this study's carbonates (from Soreq), the closed symbols represent samples of corresponding drip water and carbonates, while open symbols represent drip waters sampled elsewhere in the cave, but only compared to the same carbonates as above.

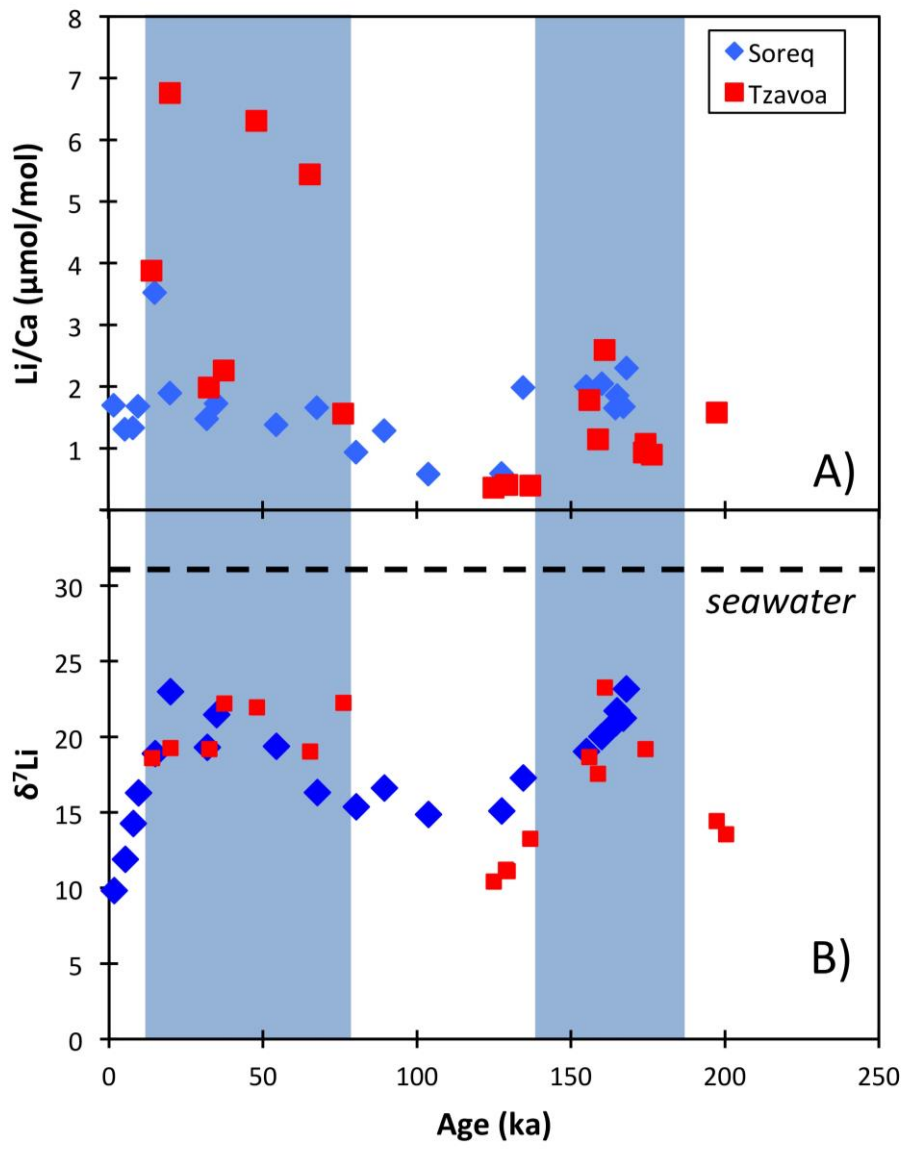


Figure 4. A) Li/Ca ratios of the speleothems compared to Li isotope ratios (B).

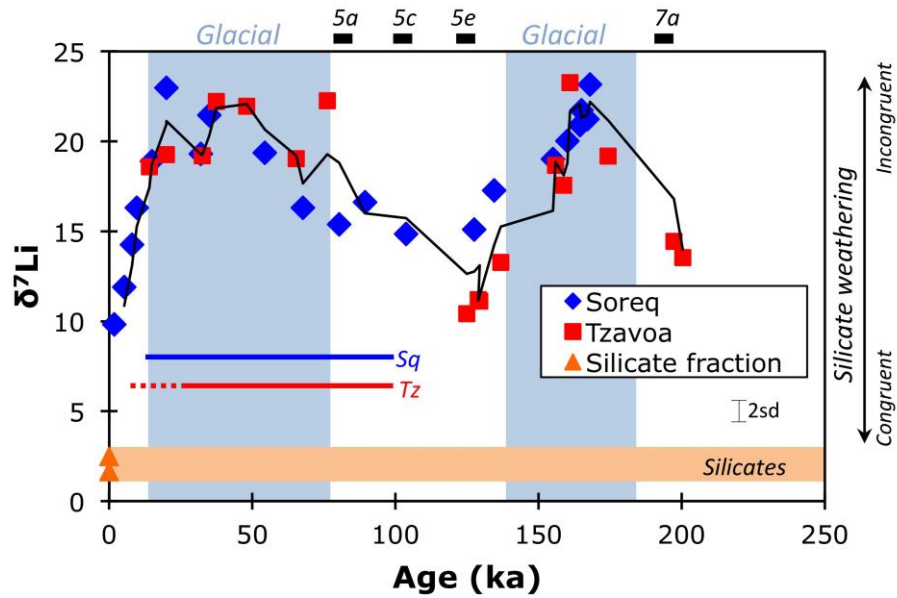


Figure 5: Lithium isotope data from speleothems in Soreq and Tzavoa caves, where the black line represents a 2-point running average. Also shown are the silicate soil $\delta^7\text{Li}$ values from both cave sites. The solid horizontal blue and red lines represent periods when soil was deposited at Soreq (Sq) (Crouvi et al., 2009) and Tzavoa (Tz) (Faershtein et al., 2016). The dotted horizontal red line represents periods when soil at Tzavoa was eroded and valleys incised (Faershtein et al., 2016). The lack of correlation between this and $\delta^7\text{Li}$ imply that silicate supply is not controlling weathering. The black bars at the top of the diagram represent MIS stages.

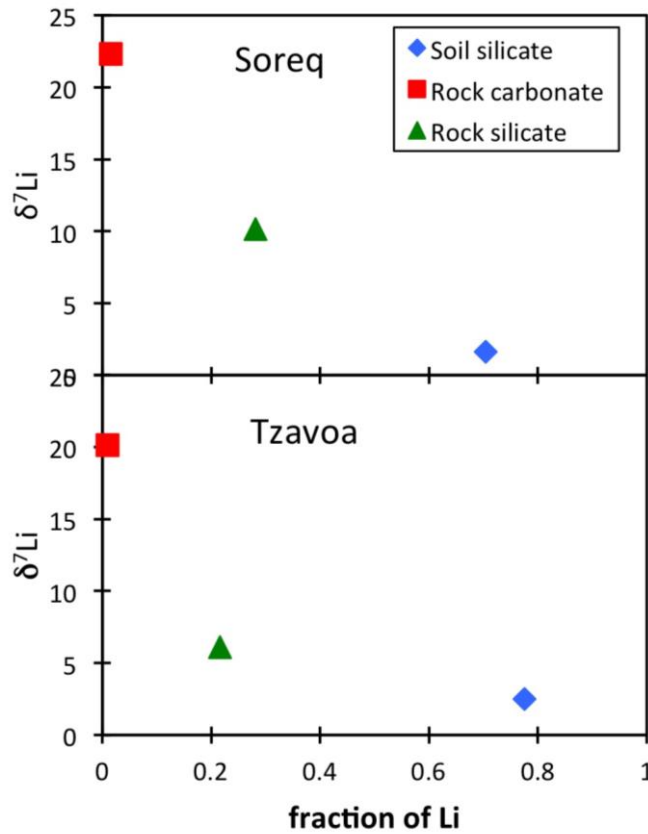


Figure 6. Li isotope composition plotted against the fraction of Li in each phase from the entire cumulative thickness of rock or soil above each cave. The soil silicate is likely an underestimate for Li available from the soil silicate fraction, because the soils contain a large proportion of high-activity primary silicates that dissolve more readily.

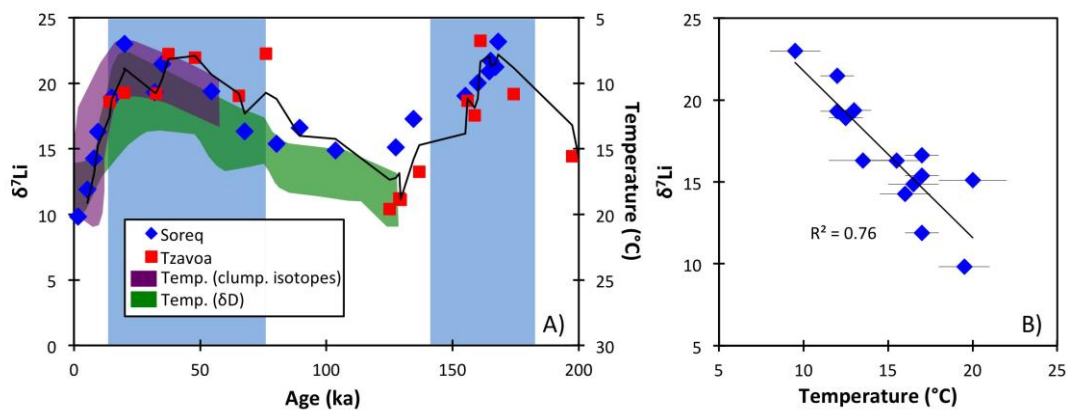


Figure 7. A) Li isotope ratios of speleothems plotted against time. Superimposed on the Li profile are palaeotemperatures from Soreq: the purple area represents temperatures data from clumped isotopes (Affek et al., 2008), whereas the green area represents data from fluid inclusion δD (McGarry et al., 2004) – note that the temperature axis is inverted. B) The correlation between $\delta^{7}Li$ and palaeotemperature for Soreq.

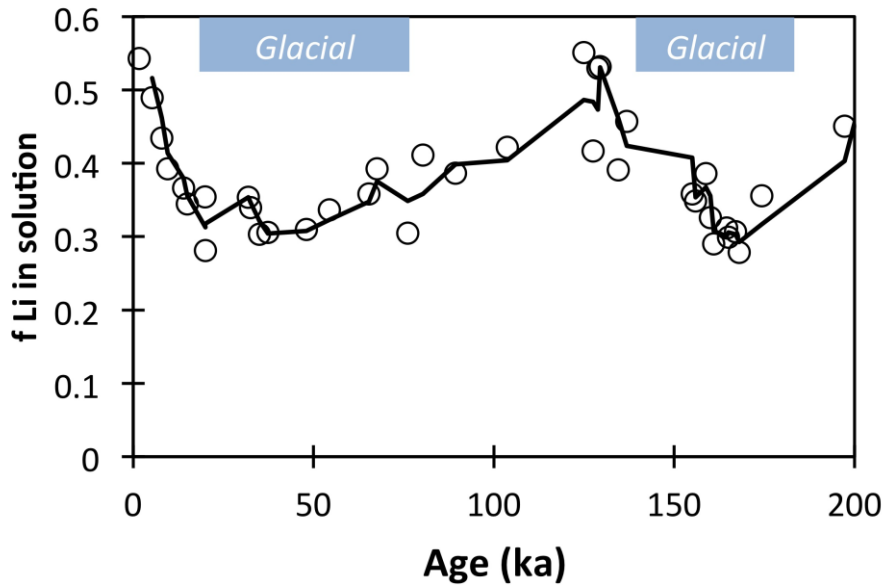


Figure 8. Silicate weathering congruency, based on calculation of the fraction of Li in solution relative to that taken into secondary weathering minerals (see text for details). Significantly more Li is in solution in the interglacials.